iVES OENO One vine & wine

DOI: https://doi.org/10.20870/oeno-one.2025.59.3.9148

OPEN ACCESS

VITICULTURE SHORT COMMUNICATIONS

Visualising xylem vessels connections formed one year after grafting using different techniques

Marilou Camboué[1*], Anne Janoueix[1], Anne-Sophie Spilmont[2], Guillaume Mathieu[2], Nathalie Ollat[1], Luis Gonzaga Santesteban[3], and Sarah Jane Cookson[1]

[1] EGFV, Univ. Bordeaux, Bordeaux Sciences Agro, INRAE, ISVV, F-33882, Villenave-d'Ornon, Bordeaux France
[2] IFV, French Institute of Vine and Wine, Domaine de l'Espiguette, Le Grau-du-Roi, France
[3] Departement of Agronomy, Biotechnology and Food Science, Univ. Pública de Navarra UPNA, Pamplona, Navarra, Spain

Article number: 9148

*correspondence:
sarah.cookson@inrae.fr

Associate editor:
Luigi Bavaresco

Received:
7 February 2025

Accepted:
7 June 2025

Published:
4 July 2025

This article is published under the **Creative Commons licence** (CC BY 4.0).

Use of all or part of the content of this article must mention the authors, the year of publication, the title, the name of the journal, the volume, the pages and the DOI in compliance with the information given above.

ABSTRACT

Grapevine grafting is an important technique in viticulture and the formation of vascular connections between the scion and rootstock is essential for successful grafting. This study aims to compare the internal tissue organisation and functional xylem vessel connections in grapevine grafts that have passed the nursery quality selection process, produced using different commonly used grafting techniques: omega, full cleft, cleft, and whip & tongue. X-ray micro-computed tomography (micro-CT), a three-dimensional imaging technique, was used to observe the anatomy of the graft union based on tissue X-ray density, and functional xylem vessels were labelled with a contrast agent. This approach allowed us to study in 3D the total volume of the graft interface, the volume of air spaces/necrotic tissues, and the distribution of functional xylem vessels. The results show that functional xylem vessels connect the scion and rootstock in all grafting types, although in some grafts, this connection is not continuous around the entire circumference of the graft interface. Grafting type did not significantly affect the proportion of air spaces/necrotic tissues relative to the graft interface volume. Omega grafts were found to be more compact, with shorter graft interfaces and, as a result, a smaller absolute volume of air spaces/necrotic tissues at the graft interface. By combining 3D morphological and functional analysis, this study provides new insights into the internal quality of grapevine grafts depending on the grafting technique used.

KEYWORDS: grafting, X-ray tomography, xylem connections, rootstock, scion, iohexol

INTRODUCTION

Grafting is an ancient horticultural practice still widely used today (Mudge *et al.*, 2009). The tissues of the scion, the aerial part, and the rootstock, the root system, are brought together to create a single individual thanks to intrinsic wound healing mechanisms. In the case of viticulture, grafting makes it possible to combine the quality of European grape berry varieties with the root phylloxera tolerance of American genotypes. The requirement to graft grapevine in most of the world has led to the development of the grapevine nurseries and their role is crucial to the wine industry.

In the book '*Le greffage de la vigne*' (Lepage, 1930), it is noted that following the phylloxera invasion, numerous grafting techniques were developed (splice, cleft, whip & tongue (W&T), chip-budding, etc.). Only a few of these grafting techniques became widespread in practice. In 1925, Mr Couderc reported that W&T grafting was the most widely used bench grafting technique at the time. He also spoke of the use of bench grafting in regions with cold, wet springs and, conversely, on site grafting in regions with rather warm springs and little rain (Chevalier, 1925).

Today, most grafts produced for viticulture are based on table-top omega grafting. Although various machines were developed as grafting became widespread, the omega technique eventually became the most popular among grapevine nursery workers. This technique, patented in 1975 and widely adopted by the 1980s, allows the scion and rootstock to be securely joined without the need for tying or binding. Additionally, it facilitates handling, enabling the industrial production of grafted grapevines. The widespread use of omega grafting has allowed the industry to meet the significant demands of the viticultural sector.

Omega grafting is carried out in one or two operations at a rate of 600 to 700 grafts per h. However, despite the success of omega grafting machines, companies are still working to developing new machines for bench grafting of grapevine, such as, Mortaise grafting (VCR nursery) and F2 grafting (Hebinger Nurseries).

A study into the two-dimensional (2D) anatomy of the graft union of grapevines produced with different techniques was recently published (Battiston *et al.*, 2022). They studied plants grafted with omega, full cleft and W&T techniques four months after grafting and found that plants grafted with the omega technique had the smallest area of necrotic tissues at the graft interface (Battiston *et al.*, 2022). However, although serial 2D sections were taken to characterise callogenesis, their 2D analysis was not sufficient to provide a complete understanding of the heterogeneity of the graft interface, since the volume of different tissues could not be calculated. Three-dimensional imaging techniques, such as X-ray micro-computed tomography (micro-CT) and magnetic resonance imaging, can overcome these limitations, having been used to study the graft interface of grapevine previously (Bahar *et al.*, 2010; Camboué *et al.*, 2024; Milien *et al.*, 2012). Moreover, in addition to characterising the structure of tissues at the graft interface, it is also important to understand their function. We recently published a new method to study functional xylem vessel connections across graft interfaces (Camboué *et al.*, 2024). This method is based on root loading of the contrast agent iohexol and its visualisation in 3D by micro-CT.

The objective of this study was to characterise the internal tissue organisation and functional xylem vessel connections in one-year-old grapevine grafts produced using different grafting techniques, in order to understand the anatomical and functional implications of each method. All grafted plants included in this study had successfully passed nursery quality selection (*i.e.*, had passed the "thumb test" and had vigorous root and shoot growth), meaning they met the quality standards required for commercialisation. This allowed us to examine whether different grafting techniques, while producing market-ready plants, result in distinct internal anatomical organisations. To do so, we used X-ray micro-computed tomography (micro-CT), a high-resolution 3D imaging technique that enables observation of internal structures. This approach enabled us to visualise and quantify tissues at the graft interface in a way that would not be possible with conventional 2D microscopy analysis. Using this method, we aimed to provide new insights into the internal quality of grafted plants and their potential long-term performance depending on the grafting technique used.

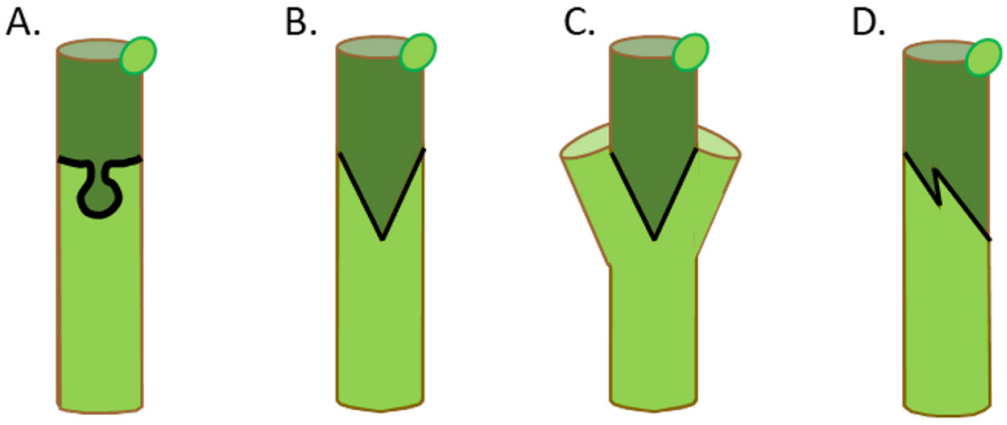


FIGURE 1. The different grafting techniques used in this study, (A) omega, (B) full cleft, (C) cleft and (D) whip & tongue.

MATERIALS AND METHODS

1. Plant material

Vitis vinifera cv. Tempranillo scions were grafted onto *V. berlandieri x V. rupestris* cv. 110 Richter rootstocks using four grafting techniques: omega, full cleft, cleft and W&T (Figure 1). These grafts were cultivated at the Vitis Navarra nursery in Navarra, Spain, during one growing season. In total, 12 grafted plants were studied: three per grafting technique. All the grafts selected were of high quality, with a mechanically resistant graft unions (having successfully passed the "thumb test"), and showed vigorous scion and rootstock growth. After uprooting in winter, the grafts were stored in perforated plastic bags at 4 °C. Roots were trimmed to 5 cm and the stems were pruned to two nodes. They were then potted in compost:sand mix (50:50, *v/v*) in 7 L pots, transferred to a greenhouse, and watered daily with tap water. When the plants had formed approximately 10 leaves, two months after transfer, the plants were used for micro-CT analysis.

2. X-ray micro-computed tomography acquisitions

X-ray micro-computed tomography (micro-CT) scans were performed using the EasyTom 150 (RX Solutions) at the Institut des Sciences de l'Évolution de Montpellier, France. The grafted plants were imaged with a spatial resolution of 29 µm voxel^{-1}, except for one sample, which was scanned at 24 µm voxel^{-1} to accommodate the larger size of the plant, ensuring it did not touch the X-ray detector. Each scan took approximately 5 min. The acquisition protocol followed the same procedure detailed in Camboué *et al.* (2024). Briefly, each grafted plant was first scanned to obtain a baseline image (T_0). Subsequently, the roots were cut underwater at approximately 2 cm from the base of the stem and immersed in pots of 100 mL containing 30 mL of a 60 mg/mL iohexol solution for 24 h and placed in a growth chamber. After this period, the plants were rescanned to capture the post-iohexol images (T_{24}). This dual time-point approach allowed us to observe functional, iohexol transporting vessel connections across the graft interface. Raw data are available at https://doi.org/10.57745/GA1OZ5.

3. Image analysis

The analysis was done using Fiji/ImageJ (ImageJ 2.14.0/1.54f; Java 1.8.0_322 [64-bit]) (Schindelin *et al*., 2012). The desktop computer used for this work, located at the Bordeaux Imaging Center (BIC) Photonic Platform, is equipped with an Intel® Xeon® Silver 4216 CPU, dual processors at 2.10 GHz, 512 GB of RAM, and a NVIDIA Quadro RTX 6000 (4095 MB) graphics card.

4. Segmentation of tissues

To compare and visualise the tissue organisation at the graft interface of different graft types, the segmentation focused on identifying key tissue types, such as xylem vessels in the wood prior to grafting, functional xylem vessels connecting the scion and rootstock, and air-filled spaces/necrotic tissues. Following the method described by Camboué *et al*. (2024), the 3D image stacks at T_0 and T_{24} for each graft were aligned using the FIJIYAMA plugin in Fiji/ImageJ (Fernandez & Moisy, 2020). All segmentations were performed on these aligned T_0 and T_{24} images. The segmentation was done on the z-slices (corresponding to transversal images of the graft interface) of the micro-CT stack as described in Camboué *et al*. (2024).

4.1 Isolation of xylem parenchyma in the wood prior to grafting

The pith region was manually delineated and excluded using the freehand selection tool in Fiji, then interpolated and applied to the entire stack. The separation between the wood that had formed before grafting and the wood that had formed after grafting was done using the same method: a region of interest (ROI) was drawn on several slices, interpolated, and applied to the entire stack, after which the outer part (post-grafting wood) was removed. This step was performed on the T_{24} images, as they enabled better visualisation of the new vessels compared to those present before grafting.

Once the pith and post-grafting wood were removed, only the area containing the vessels of the wood prior to grafting remained. An intensity threshold was applied to isolate the xylem vessels (dark areas) from the surrounding tissues. Two sub-stacks were saved: one for the vessels located below the graft point (rootstock) and another for those above (scion). After segmentation, these vessels were manually cleaned to ensure accurate identification.

The length of the graft interface was determined by visually inspecting the image stack along the z-axis to identify the uppermost and lowermost slices where the grafted area was visible. Based on the known voxel size and inter-slice spacing, the total length of the interface was calculated by multiplying the number of slices spanning this region by the z-resolution.

4.2 Isolation of xylem with iohexol

To identify functional xylem vessels transporting the contrast agent, the iohexol-labelled structures were extracted by subtracting the T_0 image from the aligned T_{24} image, as described by Camboué *et al*. (2024). These vessels were then segmented using the Waikato Environment for Knowledge Analysis/Weka plugin, and obvious artefacts were removed manually. The segmented vessels were extracted to create a binary stack. This binary stack was processed using the '3D Manager' plugin, where objects with a volume smaller than 0.05 mm^3 were first excluded, providing a supplemental cleaning step. Subsequently, using the same plugin, only the objects corresponding to xylem vessels were retained.

4.3 Segmentation of air spaces/necrotic tissues from callus/X-ray dense tissues at the graft interface

The primary objective of this step was to quantify the volume of air spaces and/or necrotic tissues (*i.e*., regions of low X-ray radiodensity) in the graft interface. To do so, the

graft interface was manually delineated on several slices of the T_0 image using the freehand selection tool in Fiji/ImageJ. The selections were managed via the ROI Manager and interpolated to generate a continuous selection throughout the stack. This selection was then converted into a binary mask representing the total volume of the graft interface. This mask was applied to the T_0 image using the Image Calculator (AND) plugin, allowing us to isolate the pixels within the graft interface. A threshold-based segmentation was then used to distinguish empty regions (dark pixels with low X-ray density) from denser areas (lighter grey pixels with higher density). As a result, two binary masks were obtained: one corresponding to the entire graft interface, and the other to low-density regions, which correspond to the volume of air spaces/necrotic tissues in the graft interface. Finally, the volumes were quantified in mm^3 using the 3D Manager plugin, applied to both binary mask. For each grafted plant, a ratio was calculated which corresponds to the volume of air spaces/necrotic tissues relative to the total graft interface volume.

4.4. Quantification of vessel connections

To quantify the extent of functional xylem vessel connections above and below the graft interface, two sub-stacks of functional xylem vessels were selected, one in the scion and one in the rootstock. Ten images (called slices in micro-CT analysis) were used, providing a volume of functional xylem vessels for a thickness of 290 µm of woody stem tissue. However, one of the cleft and W&T grafts could not be analysed, because the area scanned was too small and did not include enough undamaged rootstock to measure (Table 1). The precise slices selected for the calculation of functional xylem vessel volume in the undamaged scion and rootstock are provided in Table 1. The '3D Manager' plug-in was used to quantify the volume of these iohexol-labelled vessels, allowing the comparison of functional xylem vessel volume between different areas around the graft interface.

5. Measurements and statistical analysis

The length of the graft interface was determined by visually inspecting the image stack along the z-axis to identify the uppermost and lowermost slices where the grafted area was visible. This was based on the known voxel size and inter-slice spacing.

All graphs and statistical analysis were done with Sigm.aPlot v16, Systat Software, Inc., San Jose, California, USA.

RESULTS AND DISCUSSION

1. Functional xylem vessels connect the scion and the rootstock in all grafting types

The functional xylem vessels that transported iohexol between the rootstock and scion were found in all grafting types studied (Figure 2; Videos S1-12). Iohexol-transporting vessels were found exclusively in the newly formed wood, with no functional vessels in the xylem formed before grafting.

In some grafts, this connection was not continuous around the entire circumference of the graft interface. In the omega grafts (Figure 2A-C), functional xylem vessels were well distributed at the graft interface in one example (Figure 2A), but in the other two examples the vessels were heterogeneously distributed (Figure 2B-C). For the full cleft grafts (Figure 2D-F), functional xylem vessels encircled the entire circumference of two grafts (Figure 2E-F), whereas functional xylem vessel connections were heterogeneous in one of the grafts (Figure 2D). In general, when functional xylem vessel connection were heterogeneously distributed in omega and full cleft grafts, more functional xylem connections appeared on one side of the graft, below the bud (Videos S2, S3, and S4). In the supplementary movies, the bud can be localised thanks to the xylem vessel connections heading towards it. This highlights the positive effect buds have on graft union formation, which is presumably associated with the flow of auxin from the bud driving healing processes (Feng *et al.*, 2024; Loupit *et al.*, 2023).

In the three cleft grafts (Figure 2G-I), functional xylem vessels were only present towards the base of the scion. In the W&T grafts (Figure 2J-L), the xylem vessels were generally well distributed along the circumference of the graft interface, however, some regions had little callus tissue and fewer xylem connections (indicated by the yellow arrows, Figure 2J-K). In one of the W&T grafts, some functional xylem vessels passed through the internal part of graft interface area (Figure 2L).

2. The scion and rootstock differ in the quantity of functional xylem vessels

To quantify the extent of functional xylem vessel connections between the scion and rootstock, the volume of iohexol was calculated in 290 µm of the woody stem of the scion and rootstock for each graft. The volumes were very variable and one of the cleft and W&T grafts could not be analysed (Table 1). The volumes of iohexol transporting tissues in the rootstock and scion, and their ratios were compared for the omega and full cleft grafts, and they were not different according to a t-test. Regardless of the type of graft, the volume of iohexol (*i.e.*, functional xylem vessels) in 290 µm of woody stem was higher in the scion than in the rootstock part of the graft. This difference in the volume of functional xylem vessels could be due to genotype-specific differences between the rootstock and scion (110R and Tempranillo respectively). Xylem vessel size and density varies among grapevine genotypes (Gerin *et al.*, 2024) and our data seem to agree with the literature. Tempranillo xylem vessels have a mean diameter of 42 µm with a density of 132 vessels per mm^2 (Lamarque *et al.*, 2023), whereas xylem vessels of 110R have a mean diameter of 84 µm with 35 vessels per mm^2 (Ramsing *et al.*, 2021), this would suggest that the total conductive area of Tempranillo is twice that of 110R. This is in close agreement with our results, on average; the total conductive area in the Tempranillo scion was 1.87 times higher than the 110R rootstock.

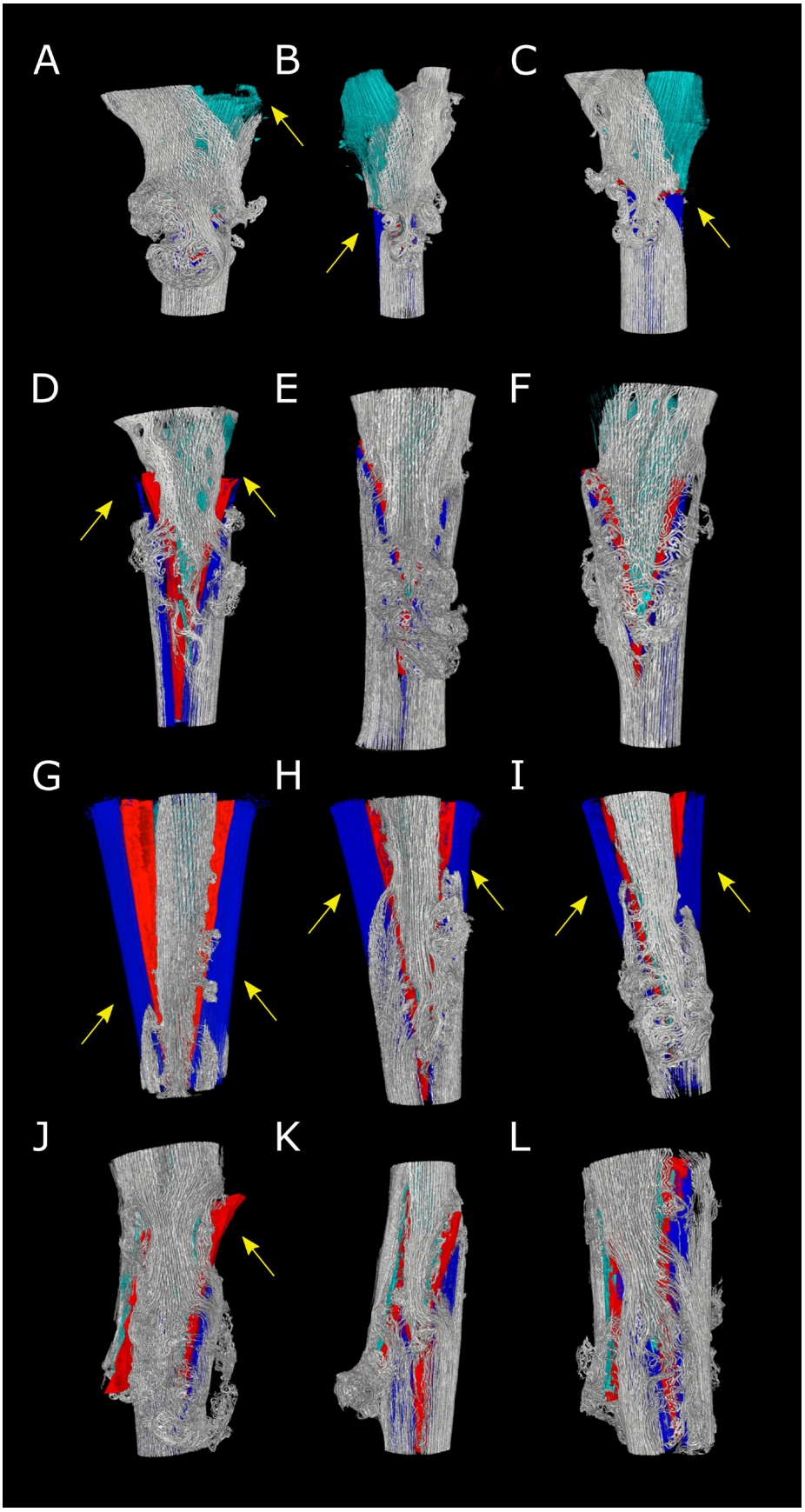


FIGURE 2. Three-dimensional reconstruction of different tissues at the graft interface of four grafting types: (A-C) omega, (D-F) full cleft, (G-I) cleft, and (J-L) whip and tongue. Functional xylem vessels labelled with iohexol shown in white. Air spaces/necrotic tissues shown in red. The scion and rootstock xylem vessels present before grafting shown in cyan and navy blue respectively.

TABLE 1. Volume of iohexol labelling of functional xylem vessels in 290 µm length of woody stem of scion and rootstock.

Stack name	Slices used for rootstock	Slices used for scion	Rootstock iohexol volume (mm^3)	Scion iohexol volume (mm^3)
Omega 1	60-69	608-617	1.69	2.614
Omega 2	244-253	774-783	0.968	1.878
Omega 3	336-345	789-798	1.698	2.541
Full cleft 1	182-191	992-1001	0.705	1.086
Full cleft 2	205-214	1180-1189	1.448	2.665
Full cleft 3	172-181	1084-1093	0.938	1.721
Cleft 2	1-10	1018-1027	1.498	1.759
Cleft 3	1-10	1212-1221	0.422	1.343
Whip & Tongue 2	1-10	1284-1293	1.327	3.658
Whip & Tongue 3	1-10	1291-1300	1.312	1.791

3. Volumes of air spaces/necrotic X-ray translucent tissues of the graft interface

The omega grafts had the lowest graft interface volume while the cleft grafts had the highest (Figure 3). This is associated with the length of the graft interface, as omega grafts were much shorter than the other types (with an average of 8.5 mm); this was followed by full cleft (27.1 mm) and W&T (29.3 mm), and then cleft being the longest (35.6 mm) (Table 2). The volume of air spaces/necrotic tissues at the graft interface show some variation between graft types, although this difference is not statistically significant (Figure 3). Battiston *et al*. (2022) measured the area of necrosis on 2D images of omega, full cleft and W&T grafts and found that full cleft grafts often had the highest amount of necrosis (although this depended on the scion/rootstock combination). We observed the same tendency, with higher air space/necrotic tissues in full cleft than omega grafts. The slight differences between our work and Battiston *et al.* (2022) could be because the X-ray tomography equipment that we used cannot distinguish air spaces from X-ray translucent necrotic tissues, whereas Battiston *et al.* (2022) used classical histology, which can easily identify necrotic tissues. Although there are some advantages of classical histology, these techniques are invasive and do not allow 3D volumes to be accurately calculated.

In addition to measuring absolute volumes, we calculated the ratio of the volume of air spaces/necrotic tissues to the volume of the graft interface (Figure 4) to provide a clearer comparison between graft types. We found that the proportion of air spaces/necrotic tissues relative to the graft

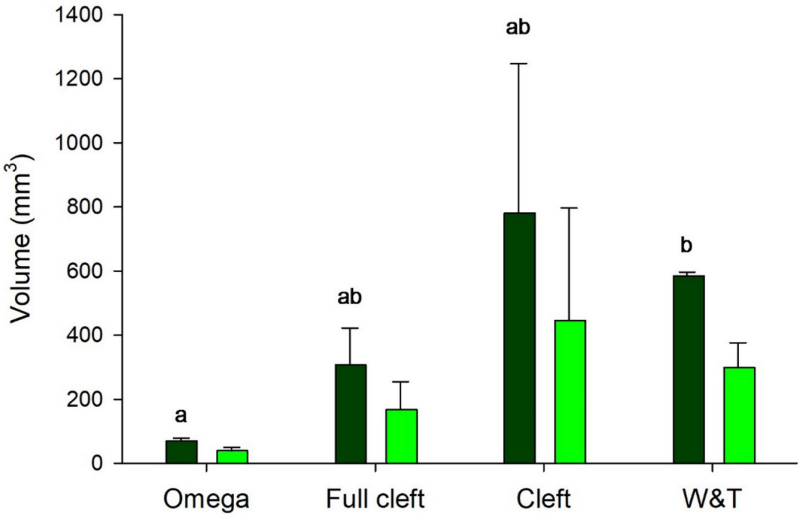


FIGURE 3. Volume of the whole graft interface (dark green) and air spaces/necrotic tissues (light green) in grapevine grafted with different techniques. Mean and standard deviations shown (n = 3). Letters indicate the results of a Tukey test after an ANOVA on Ranks test (p = 0.033) of the whole graft interface volume. The differences between the volume of air spaces/necrotic tissues was not statistically significant (p = 0.118).

TABLE 2. Length of the graft interface of different grafting types.

	Length of graft interface (mm)
Omega	8.52b ± 0.05
Full cleft	27.18a ± 4.0
Cleft	35.69a ± 3.3
Whip & Tongue	29. 40a ± 4.6

Means and standard deviations shown (n = 3). Letters indicate the results of a Tukey test after a one-way ANOVA (p = <0.001).

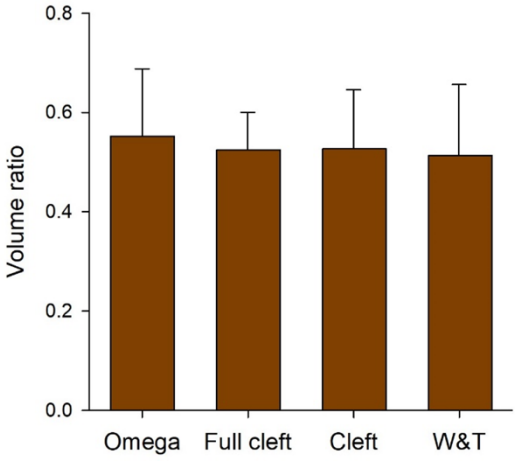


FIGURE 4. Ratio of the volume of air spaces/necrotic tissues by whole graft interface in grapevine grafted with different techniques. Mean and standard deviations shown (n = 3).

interface volume was not affected by grafting type, and that air spaces/necrotic tissues made up approximately 50 % of the volume at the grafting interface. Considering that all the grafts passed the "thumb press" test, this indicates that air spaces/necrotic tissues occupying 50 % of the graft interface does not seem to affect the success of this mechanical test. It would be interesting to compare these findings with grafts that fail the "thumb press" test or with poor mechanical resistance to determine at which percentage air spaces/necrotic tissue affect the mechanical resistance of grafted grapevine plants. It is generally assumed that the mechanical resistance of the graft interface is linked to the formation of xylem vessel connections between the scion and rootstock (Loupit *et al.*, 2023; Thomas *et al.*, 2023), but there is little experimental evidence to support this.

Grafting wounds are vulnerable to contamination by trunk diseases (Gramaje *et al.*, 2018) and it has been suggested that grafting type can affect the appearance of the esca symptoms many years after grafting (Mary *et al.*, 2017). In the study of Mary *et al.* (2017), grapevines grafted with W&T, full cleft and omega techniques were compared and the full cleft appeared to have fewer esca symptoms than the other two grafting types. However, because field data was analysed from existing commercial vineyards, plant age varied considerably between the different grafting types, making conclusions about the consequences of different grafting types difficult. One of the possible explanations for the effect of grafting type on esca symptoms is that the volume of air spaces/necrotic tissues is high in omega grafts than full cleft grafts. However, neither our data nor the work of Battiston *et al.* (2022) support this hypothesis.

CONCLUSIONS

This study highlights the morphological and functional characteristics of some grapevine grafts made using different techniques. We explored the graft interface length and volume, and the presence of air spaces/necrotic tissues and functional xylem vessels between the scion and rootstock. For the first time, different types of grafts were studied in three dimensions using micro-CT; this innovative approach provides a good understanding of internal tissue structures. This work highlighted the complexity and heterogeneity of functional xylem vessel connections between the scion and rootstock at the graft interface. Approximately 50 % of the graft interface volume is non-functional (air spaces or necrotic tissues) in all grafting types, yet this does not appear to affect the mechanical resistance of the graft union (tested using the thumb test). In the future, it would be interesting to analyse older plants, as it is possible that poor xylem connections subsequently improve during the life of grafted plants in the vineyard.

ACKNOWLEDGEMENTS

This work was funded with the project EFA 324/19 - VITES QUALITAS and EFA033/01 - VITRES, 65 % co-funded by the European Regional Development Fund (FEDER) through the Interreg Program V-A Spain-France-Andorra (POCTEFA 2014-2020 and POCTEFA 2021–2027, respectively). Micro-CT acquisitions were performed in Montpellier, France, at the MRI platform, member of the national infrastructure France-BioImaging and supported by the French National Research Agency (ANR-10-INBS-04, "Investments for the Future"), and member of the Labex CEMEB (ANR-10-LABX-0004) and NUMEV (ANR-10-LABX-0020). Authors warmly thank Renaud Lebrun (CNRS) for technical assistance with micro-CT. The micro-CT image analysis was done in the Bordeaux Imaging Center, a service unit of the CNRS-INSERM and Bordeaux University, a member of France BioImaging, with the help of Jérémie Teillon and Fabrice Cordelières. The authors also thank Javier Eraso, Ana Villa-Llop and Rafael García from Vitis Navarra nursery and Maria Lafargue, Cyril Hevin and Nicolas Hocquard from the EGFV for their contributions.

REFERENCES

Bahar, E., Korkutal, I., Carbonneau, A., & Akcay, G. (2010). Using magnetic resonance imaging technique (MRI) to investigate graft connection and its relation to reddening discoloration in grape leaves. *Journal of Food, Agriculture & Environment*, *8*((3&4)), 293-297. https://doi.org/https://doi.org/10.1234/4.2010.3149

Battiston, E., Falsini, S., Giovannelli, A., Schiff, S., Tani, C., Panaiia, R., […] & Mugnai, L. (2022). Xylem anatomy and hydraulic traits in Vitis grafted cuttings in view of their impact on the young grapevine decline [Original Research]. *Frontiers in Plant Science*, *13*. https://doi.org/10.3389/fpls.2022.1006835

Camboué, M., Janoueix, A., Tandonnet, J.-P., Spilmont, A.-S., Moisy, C., Mathieu, G., […] & Cookson, S. J. (2024). Phenotyping xylem connections in grafted plants using X-ray micro-computed tomography. *Plant, Cell & Environment*, *47*(7), 2349-2359. https://doi.org/https://doi.org/10.1111/pce.14883

Chevalier, A. (1925). L'amélioration de la vigne en France et les Travaux de G. Couderc sur l'Hybridation et le Greffage. *Journal d'agriculture traditionnelle et de botanique appliquée*, *5*(51), 809-840. https://doi.org/10.3406/jatba.1925.4341

Feng, M., Augstein, F., Kareem, A., & Melnyk, C. W. (2024). Plant grafting: Molecular mechanisms and applications. *Molecular Plant*, *17*(1), 75-91. https://doi.org/10.1016/j.molp.2023.12.006

Fernandez, R., & Moisy, C. (2020). Fijiyama: a registration tool for 3D multimodal time-lapse imaging. *Bioinformatics*, *37*(10), 1482-1484. https://doi.org/10.1093/bioinformatics/btaa846

Gerin, D., Chimienti, N., Agnusdei, A., Mannerucci, F., Angelini, R. M. D., Faretra, F., & Pollastro, S. (2024). Xylem Vessel Size Is Related to Grapevine Susceptibility to Phaeomoniella chlamydospora. Horticulturae, 10(7), Article 750. https://doi.org/10.3390/horticulturae10070750

Gramaje, D., Úrbez-Torres, J. R., & Sosnowski, M. R. (2018). Managing Grapevine Trunk Diseases With Respect to Etiology and Epidemiology: Current Strategies and Future Prospects. *Plant Disease*, *102*(1), 12-39. https://doi.org/10.1094/pdis-04-17-0512-fe

Lamarque, L. J., Delmas, C. E. L., Charrier, G., Burlett, R., Dell'Acqua, N., Pouzoulet, J., […] & Delzon, S. (2023). Quantifying the grapevine xylem embolism resistance spectrum to identify varieties and regions at risk in a future dry climate. *Sci Rep*, *13*(1), 7724. https://doi.org/10.1038/s41598-023-34224-6

Lepage, E. (1930). *Le greffage de la vigne*. Paris, J.-B. Baillière.

Loupit, G., Brocard, L., Ollat, N., & Cookson, S. J. (2023). Grafting in plants: recent discoveries and new applications. *Journal of Experimental Botany*, *74*(8), 2433-2447. https://doi.org/10.1093/jxb/erad061

Mary, S., Laveau, C., Lecomte, P., Birebent, M., & Roby, J.-P. (2017). Impact of grafting type on Esca foliar symptoms. *OENO One*, *51*(3). https://doi.org/10.20870/oeno-one.2016.50.4.1408

Milien, M., Renault-Spilmont, A. S., Cookson, S. J., Sarrazin, A., & Verdeil, J. L. (2012). Visualization of the 3D structure of the graft union of grapevine using X-ray tomography. *Scientia Horticulturae*, *144*, 130-140. https://doi.org/10.1016/j.scienta.2012.06.045

Mudge, K., Janick, J., Scofield, S., & Goldschmidt, E. E. (2009). A History of Grafting. *Horticultural Reviews*, *35*, 437-493. https://doi.org/10.1002/9780470593776.ch9

Ramsing, C. K., Gramaje, D., Mocholi, S., Agusti, J., Cabello Saenz de Santa Maria, F., Armengol, J., & Berbegal, M. (2021). Relationship Between the Xylem Anatomy of Grapevine Rootstocks and Their Susceptibility to Phaeoacremonium minimum and Phaeomoniella chlamydospora. *Front Plant Sci*, *12*, 726461. https://doi.org/10.3389/fpls.2021.726461

Schindelin, J., Arganda-Carreras, I., Frise, E., Kaynig, V., Longair, M., Pietzsch, T., […] & Cardona, A. (2012). Fiji: an open-source platform for biological-image analysis. *Nature Methods*, *9*(7), 676-682. https://doi.org/10.1038/nmeth.2019

Thomas, H. R., Gevorgyan, A., & Frank, M. H. (2023). Anatomical and biophysical basis for graft incompatibility within the Solanaceae. *Journal of Experimental Botany*, *74*(15), 4461-4470. https://doi.org/10.1093/jxb/erad155